ELSEVIER

Journal of Power Sources 114 (2003) 127–132

JOURNAL OF POWER SOURCES

www.elsevier.com/locate/jpowsour

Synthesis of $LiCoO_2$ by metallo-organic decomposition-MOD

S.M. Lala, L.A. Montoro, E. di Donato, J.M. Rosolen*

Departamento de Química, FFCLRP, Universidade de São Paulo, 14040-901 Ribeirão Preto, SP, Brazil

Received 22 September 2002; accepted 30 September 2002

Abstract

We have studied the preparation of $LiCoO_2$ powder using the metallo-organic decomposition (MOD) route in air. Cobalt and lithium 2-ethylhexanoate were obtained from hydroxides and 2-ethylhexanoic acid. TG/DTA and XRD techniques were used to study the steps of formation of well-organized $LiCoO_2$ (*R-3m*). The MOD route produced $LiCoO_2$ (*R-3m*) at 700 °C with specific surface area 1.7 $m^2\ g^{-1}$ and grain size distribution $d_{50} = 24$ μm. The electrochemical response of MOD $LiCoO_2$ powder was tested by cyclic voltammetry and discharge/charge cycles in a composite electrode. The MOD method yields $LiCoO_2$ agglomerated particles with size distribution and porosity that facilitate lithium diffusion in the composite electrode.

Keywords: $LiCoO_2$ powder; Li-ion batteries; Metallo-organic decomposition

1. Introduction

The synthesis method of lithiated metal oxides used in Li-ion batteries has a fundamental role in electrochemical performance. The choice of starting materials and the preparation conditions can determine the grain size distribution, morphology and purity of materials; features that have a strong influence in Li-ion battery performance (capacity fade, rate of charge/discharge).

The high temperature HT-$LiCoO_2$ compound is a p-semiconductor oxide that has been widely studied because of its role in the lithium ion battery [1–19]. The reversible specific capacity of HT-$LiCoO_2$ is about 145 mAh g^{-1} and its the specific energy ca. 1070 Wh kg^{-1} based on an average discharge voltage of 3.9 V. The main precursors employed in the HT-$LiCoO_2$ synthesis have been cobalt and lithium nitrate, carbonate, acetate or hydroxide. Several preparation routes have been developed and studied using these precursors associated sometimes with chelating agents for production of HT-$LiCoO_2$ [3–5,9,20–35]. All these studies have shown that the precursors have a great influence on the temperature and time of sintering, grain size distribution, aggregation and morphology of HT-$LiCoO_2$ particles. For example, methods like decomposition of hydroxides [25], Pechini [27], electrostatic spray [30], sol–gel [31] and hydrothermal conditions [32] are able to provide well-ordered $LiCoO_2$ grains at temperatures and reaction times lower than the carbonate method. Preparation of $LiCoO_2$ at 300 °C has been achieved from hydroxide mixture and at 400 °C from either cobalt nitrate [33] or Co acetate [34].

The MOD route is another method that can be used to produce oxides. It has been particularly useful in the processing of ferroelectric and electro-optic thin films [35–37], but not for the synthesis of the Li oxide materials such as $LiCoO_2$. In this paper, we study the MOD method for the synthesis of HT-$LiCoO_2$ using metallo-organic precursors obtained from hydroxides and 2-ethylhexanoic acid. The main characterization techniques were TGA/DTA, XRD, BET, cyclic voltammetry and charge/discharge galvanostatic. The electrochemical quality of oxide was investigated using composite electrodes. It was found that MOD HT-$LiCoO_2$ fired at 700 °C is adequate for the preparation of a composite electrode with high lithium diffusion. This high lithium diffusion was attributed to porosity in the MOD HT-$LiCoO_2$ agglomerate particles.

2. Experimental

Lithium and cobalt 2-ethylhexanoate were obtained from the acid–base reaction between 2-ethylhexanoic acid (Alfa-Aesar, $(CH_3(CH_2)_3(C_2H_5)COOH)$, 99.9%)) and lithium or

* Corresponding author. Tel.: +55-16-602-3787; fax: +55-16-633-8151.
E-mail address: rosolen@ffclrp.usp.br (J.M. Rosolen).

0378-7753/02/$ – see front matter
PII: S0378-7753(02)00590-6

cobalt hydroxides (Fluka, $Li(OH)\cdot H_2O$, 99% and Alpha-Aesar, $Co(OH)_2$, 99%). The reaction $nCH_3(CH_2)_3(C_2H_5)$-$COOH + M(OH)_n \rightarrow [CH_3(CH_2)_3(C_2H_5)COO]_nM + nH_2O$ was carried out under reflux conditions (room atmosphere) at 110 °C for 4 h. The molar proportion of acid and base dissolved in THF was 2:1 for the $[CH_3(CH_2)_3(C_2H_5)$-$COO]_2Co^{2+}$ and 1:1 for the $[CH_3(CH_2)_3(C_2H_5)COO]Li^{1+}$ salts. All metallo-organic compounds were dried under vacuum (9.5×10^4 Pa) at 80 °C.

To study the preparation of MOD HT-$LiCoO_2$ in air the lithium and cobalt 2-ethylhexanoate salts were mixed in molar proportions of 2:1. The solvent used to mix the two metallo-organic compounds was tetrahydrofuran (THF). The crucible used in the sintering of the HT-$LiCoO_2$ and for successive heating of the metallo-organo solution, was alumina. An excess of lithium salt was used because of evaporation of the lithium salts and its reaction with the alumina crucible.

Thermogravimetric/differential thermal analysis (TGA/DTA) was performed in synthetic air for the two precursors and its mixture (heating rate 10 °C min^{-1}) using a TA Instruments (model SDT-2960 Simultaneous Analyser). XRD patterns were collected using a SIEMENS D5005 diffractometer (Cu Kα radiation, graphite monochromator, range 15–75°, steps of 0.02°, and 8 s/step). The grain size distribution was measured using a particle size analyzer (Mastersize 2000). The specific surface area was measured by the Brunauer–Emmett–Teller (BET) method with N_2 (NOVA 1200).

The $LiCoO_2$ electrochemical response, was obtained using composite electrodes (8 mm diameter) at room temperature. Composite electrodes were prepared with poly(-vinylidene fluoride) binder (Solvay, 12 wt.%), carbon (Ketjen Black, MMB, 18 wt.%) and graphite (Fluka, 3 wt.%) and $LiCoO_2$ sintering at 700 °C (8 h in air). For complete mixing of active material, binder and carbon we used acetone and ultrasonic agitation. The binder was previously dissolved in acetone and then the carbon and active material were added to the polymeric solution, respectively. The slurry obtained was spread on Al foil and after solvent evaporation at atmosphere the electrode foil was hot pressed

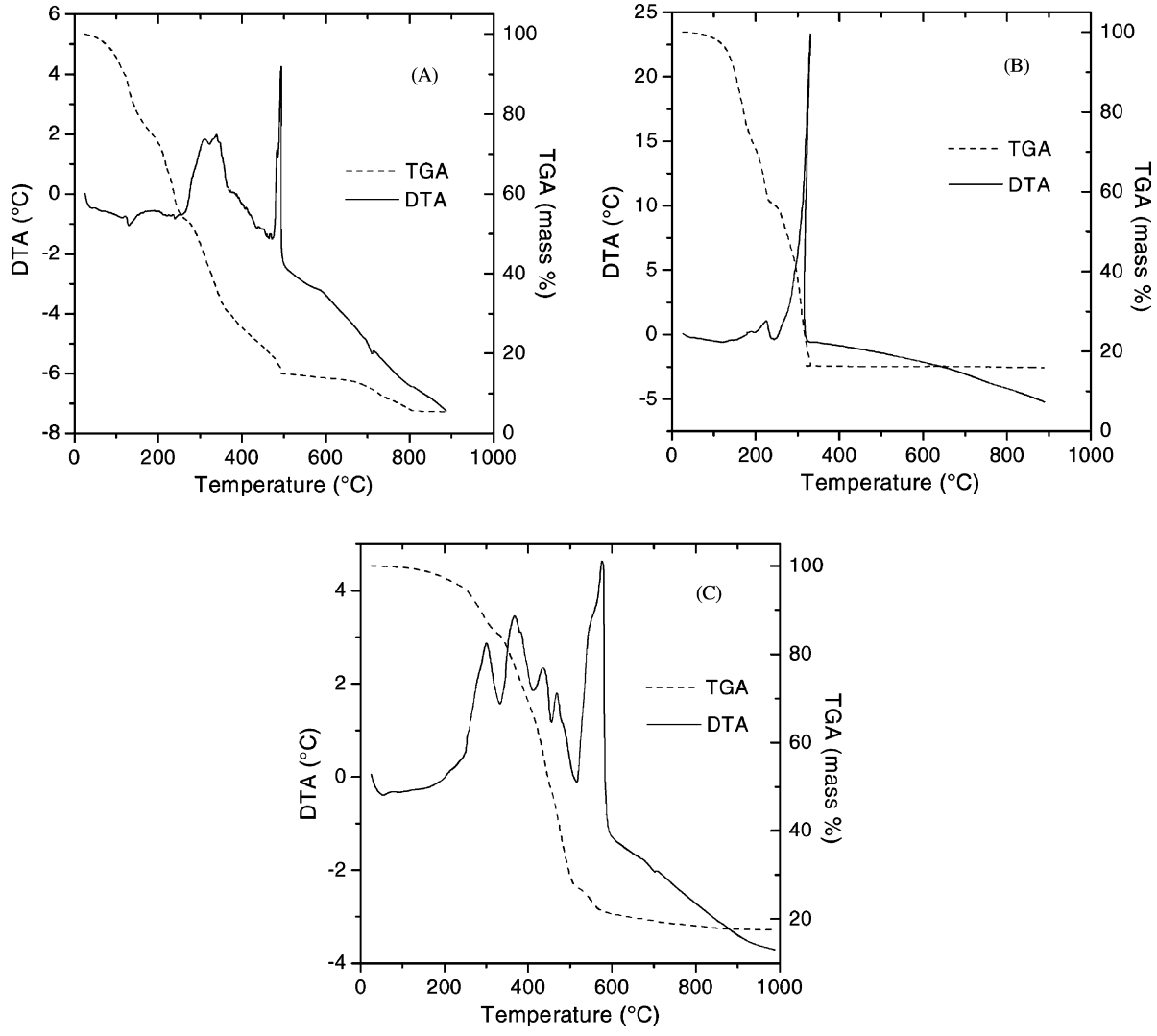

Fig. 1. TG/DTA curves for the lithium 2-ethylhexanoate (A), cobalt 2-ethylhexanoate (B) and its mixture (C).

(1.0×10^7 Pa, 120 °C). Before assembly of the electrochemical cell in a dry-box (with Ar–H_2O <3 ppm), the electrodes were heated at 120 °C under vacuum for complete removal of solvent and H_2O traces. The electrolyte used in the electrochemical characterization was a 1.0 mol. L^{-1} solution of $LiPF_6$ in dimethyl carbonate, diethyl carbonate, propylene carbonate (Selectipur—3:1:1 w/w). The cell was sealed with O-rings and it was used as separators (Celgard-Hoeschst Celanese 2400) between the electrodes. The reference and auxiliary electrodes were lithium foil (Aldrich). The discharge/charge cycles were controlled by a potentiostat/galvanostat-MacPile and the voltammetry was carried out using a PAR 362.

3. Results and discussion

Fig. 1 shows TGA/DTA curves collected for the lithium 2-ethylhexanoate (Fig. 1A), cobalt 2-ethylhexanoate (Fig. 1B) and salts mixture (Fig. 1C) utilized to synthesise the $LiCoO_2$. All curves present several steps of weight loss with peaks in the DTA curve. These thermal events have been identified by characterization of the intermediates obtained at different temperatures using X-ray diffraction.

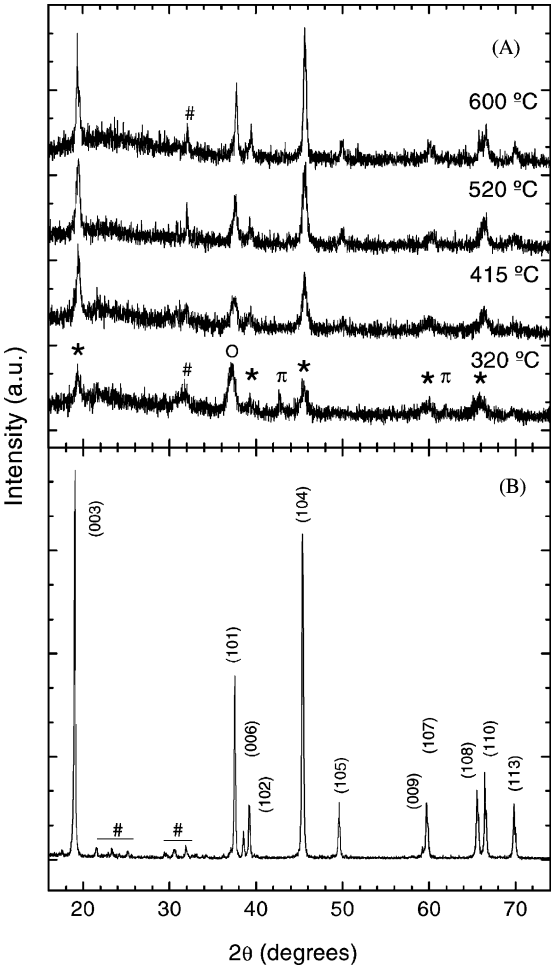

Fig. 2. (A) XRD patterns collected at room temperature for successive heatings in air (rate 5 °C min^{-1}, 3 h for each heating) for the metallo-organic mixture. Labels indicate the oxide phases: (∗) LT-Li_xCoO_2, (O) Co_3O_4, (π) CoO and (#) Li_2CO_3; (B) XRD pattern of $LiCoO_2$ obtained from MO mixture calcined at 700 °C in air (8 h).

For the lithium 2-ethylhexanoate the steps from ambient temperature to 250 °C are associated with weight loss of about 45% that is due to evaporation of THF solvent and possible dehydration of the precursor. These processes are accompanied by overlapping endothermic effects at 129 and 240 °C on the DTA curve (Fig. 1A). The steps from 240 to 500 °C are ascribed to the decomposition of the organic chain of 2-ethylhexanoate. The total weight loss in this range of temperatures associated with an exothermic process (310, 340 and 461 °C) was 34%. This value is in agreement with theoretical weigh loss that is 35%, while the small loss at 500 °C is due to the reaction of residual carboxilate groups (COOLi). The residual carboxilate groups react with air producing CO_2 and Li_2CO_3 (checked by XRD spectrum collected for lithium precursor heated at 500 °C). Fig. 1 reveals the formation of a eutectic mixture Li_2CO_3/Li_2O. The small endothermic peak at 710 °C is the fusion point of Li_2CO_3 (beginning of decomposition of Li_2CO_3 in Li_2O).

For the cobalt 2-ethylhexanoate from ambient temperature to 183 °C, evaporation of residual THF (an endothermic event) corresponds to a weight loss of about 25%. The decomposition of the carboxilate group (two steps, exothermic) occurs in the temperature range between 183 and 240 °C producing CO_2, Co_3O_4 and CoO (Fig. 2). The weight loss in this range was 15%, a value that is in agreement with the theoretical calculation, i.e. 16%. As in the case of Fig. 1A, Fig. 1B had also one intense exothermic peak. However, this exothermic peak (range 240–331 °C) is due to the decomposition of residual organic chains. This reaction accounts for 40% of weight loss and the precursor is completely converted to Co_3O_4.

Fig. 1C shows the TGA/DTA curves of the mixture of cobalt and lithium in a molar proportion of 1:2. The weight loss of metallo-organic (MO) precursor mixture occurs in three steps, at 21–310, 310–515 and 515–596 °C, and terminates at 596 °C. The weight loss in these steps corresponds to the removal of water, THF (endothermic region of Fig. 1C), combustion of organic phase and formation of oxides. As in the Fig. 1A, the TGA/DTA curves of mixture contain also the endothermic peak at 710 °C the fusion point of Li_2CO_3. The Fig. 2A shows the X-ray diffraction (XRD) patterns of product resulting from heatings of a mixture of cobalt and lithium 2-ethylhexanoate at temperatures where we observed more intense exothermic peaks. In the first exothermic peak (320 °C) the oxide phases observed are the low temperature LT-Li_xCoO_2 [38], Co_3O_4, CoO and Li_2CO_3. The next exothermic peaks were associated with the increasing LT-Li_xCoO_2 phase (415, 520 °C) and also the beginning of a phase transition LT-$LiCoO_2$ → HT-$LiCoO_2$ (600 °C). The Bragg intensity of the (0 0 3) line increased and there was splitting between the (0 0 6)/(1 0 2) and (1 0 8)/(1 1 0) lines (Fig. 2B).

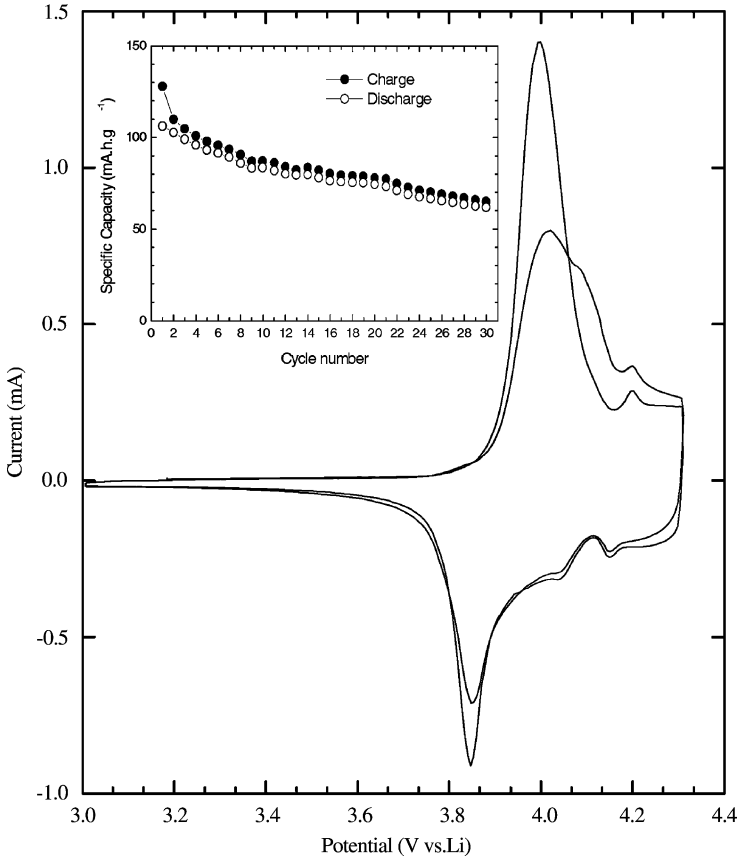

Fig. 3. Voltammogram (scan-rate 0.2 mV s^{-1}) and specific capacity vs. cycle number (charge/discharge 0.1 mA cm^2) of the composite electrode prepared with MOD HT-$LiCoO_2$. The cut-off voltage limit in both experiments was 3.0–4.3 V.

These results suggest that the MOD method allows the preparation of HT-$LiCoO_2$ at a in lower synthesis temperature and shorter times than the solid-state reaction where the calcination temperature is usually 800–1000 °C. This occurs because for the MOD route, the mixture of precursors is homogeneous an atomic scale. Besides the MO precursors can provide a mixture with high viscosity—a property that is expected to minimize the cation segregation. For the MOD route utilized in the preparation of HT-$LiCoO_2$, the precursors are completely soluble in THF. The formation of lithium and cobalt carbonates nanoparticles at a very low temperature is expected. The transition metal carbonates decompose easily to metallic oxides and CO_2 at a temperature lower than 320 °C. Furthermore, the diffusion length of the lithium and cobalt salt particles (oxides and/or carbonates) is very short, such that the system reaches thermodynamic equilibrium quickly after the organic radicals are pyrolyzed. This condition favors the formation of well crystalline HT-$LiCoO_2$. In fact, the Fig. 2B shows that the calcination of an MO mixture at 700 °C for sufficient time (8 h) yields 1.4 g of HT-$LiCoO_2$ with full crystallinity. For this HT-$LiCoO_2$ (700 °C) was evaluated the grains size distribution $d_{10} = 7.3$ μm, $d_{50} = 24$ μm and $d_{90} = 61$ μm. The specific surface area was 1.7 m^2 g^{-1}, total pore volume 1.4×10^{-3} cm^3 g^{-1} and cell parameters $a = 2.81$ Å and $c = 14.05$ Å (space group *R-3m*).

The electrochemical quality of MOD HT-$LiCoO_2$ calcined at 700 °C without post treatments (sieving, grinding, rinsing to remove the carbonate) was probed by using cyclic voltammetry and charge/discharge cycles. Fig. 3 shows the voltammogram and specific capacity versus cycle number (inset figure) of MOD HT-$LiCoO_2$ composite electrode between voltage limits where the structural alterations and electrolyte does not affect the reversible capacity of the electrode at room temperature.

The voltammogram (Fig. 3) shows during first insertion/deinsertion cycles, the two anodic (3.99, 4.19 V) and cathodic peaks (4.15, 3.84 V) and a small shoulder (4.04 V) in the cathodic scan. With increasing intercalation cycles, the intensity of these oxi-reduction peaks decrease, but they remain in the same position and very well defined at a scan-rate 0.2 mV s^{-1}.

The peaks in the voltammograms of lithium intercalation electrodes are associated with different lithium occupation sites and Li diffusion in the electrode. Alterations in the position and profile of the peaks can be thus correlated with structural modifications in the host and kinetics of intercalation. For $LiCoO_2$, the two cathodic and anodic peaks detected

are associated with reversible phase transitions. The difference of potential peaks in the voltammogram is about 50 mV, a value that is near a Nernstian reversible system. The reduction in the intensity of the peaks indicates in this case a reduction in the quantity of lithium inserted or deinserted in the active compound HT-$LiCoO_2$. For composite electrodes prepared with $LiCoO_2$ it is hard to observe the peaks in the voltammogram of Fig. 2. Often anodic/cathodic peaks, as observed in Fig. 2, are found only in $LiCoO_2$ thin film electrodes or in a voltammogram of composite electrodes performed at lower scan-rates (<0.1 mV s^{-1}). Therefore, the voltammogram with the scan-rate 0.2 mV s^{-1} is suggesting that the MOD HT-$LiCoO_2$ powder is an agglomerate of particles that facilitate lithium diffusion in the composite electrode.

Fig. 3 shows also the behavior of specific capacity in low rate for cycles of charge/discharge of MOD HT-$LiCoO_2$. The curve was obtained at a rate *C*/5 using a current density 26 mA g^{-1}. The first cycle represents a capacity in first charge of 129 mAh g^{-1} (approximately $x = 0.5$ in $Li_{1-x}CoO_2$), while the discharge capacity is 106 mAh g^{-1}. With increasing cycle number this irreversibility disappears, but the reversible specific capacity decreases.

The grain size distribution and porosity of grains (mesopore, micropore, macropore) have an important role in the performance of composite electrodes used in commercial batteries. The dispersion of materials used in the preparation of a composite electrode depends upon several parameters (size distribution particle, shape, interaction forces, etc.) that affect the mixing efficiency. The rate of charge/discharge and the capacity fade of the composite electrode depend on the mechanical stress of the electrode during polarization that may reduce the ohmic contact of the electrode [39] and the lithium diffusion when structural factors (phase transitions, chemical decomposition, disorder, etc.) are excluded. Capacity fade appears when the ohmic contacts between grains become poor because of stress associated with Li intercalation and polarization of electrode.

The high Li diffusion observed in Fig. 3 would thus be associated with porosity in MOD HT-$LiCoO_2$ particle agglomerates, possibley the shape of pores and/or the presence of micropores on surface that was not detected by the desorption isotherm used by the BET equipment. The significant volume contraction that is often observed in the grains of thin films prepared with the MOD route might have been the cause of this special porosity.

Voltammograms at the same scan-rate as Fig. 3 were also performed for composite electrode, prepared under the same conditions (binder, carbons, weigh proportion, hot press, drying), but using a HT-$LiCoO_2$ with $d_{10} = 0.31$ μm, $d_{50} = 3.14$ μm and $d_{90} = 6.30$ μm, specific surface area 7.4 $m^2\,g^{-1}$ and total pore volume 6.3×10^{-3} $cm^3\,g^{-1}$. It was observed for this HT-$LiCoO_2$ only one broad anodic and cathodic peak, instead of the two cathodic and anodic peaks of Fig. 3. Details of preparation of this HT-$LiCoO_2$ with this narrow grain size distribution and high surface area will be published elsewhere.

Besides the encouraging result observed in the voltammogram, the composite electrode prepared with micro grains of MOD HT-$LiCoO_2$ yielded a large capacity fade that was associated with losts of ohmic contact in the electrode due the mechanical stress that is generated during the polarization of electrode. This problem could be overcome best with technical parameters used in the preparation of the electrode composite [40].

4. Conclusions

The MOD route is an alternative method to obtain a well-organized $LiCoO_2$ powder. MOD HT-$LiCoO_2$ can be obtained at 700 °C and the MOD LT-$LiCoO_2$ at about 400 °C. The metallo-organic salts used were lithium and cobalt 2-ethyl hexanoate that are stable at room condition. To obtain this salts we used 2-ethyl hexanoic acid and lithium cobalt hydroxides. With these precursors and the solvent used we did not observe phase segregation. The pollutant generated during the preparation of the oxide was CO_2. The electrochemical characterization suggests that MOD HT-$LiCoO_2$ powder calcined at 700 °C consists of aggregate particles that permit the preparation of composite electrodes with facile lithium diffusion. The BET analysis and the cyclic voltammetry technique have suggested that this facile lithium diffusion might be associated with shape and pore distribution in the grains. A further study in order to investigate the shape and pore distribution is required. The MOD route studied here can be easily extended to the preparation of other lithiated oxides.

Acknowledgements

This work was supported by FAPESP (96/05347-1), CNPq/PADCT (620238/97, 301493/95-2). E. Di Donato, S.M. Lala and L.A. Montoro thank FAPESP, CNPq, Capes for Ph.D. and under-graduation fellowship.

References

[1] J.N. Reimers, W. Li, E. Rossen, J.R. Dahn, Solid State Ion. 62 (1993) 53.
[2] J.N. Reimers, J.R. Dahn, J. Electrochem. Soc. 139 (1992) 2091.
[3] G.G. Amatucci, J.M. Tarascon, L.C. Klein, J. Electrochem. Soc. 143 (1996) 1143.
[4] T. Ohzuku, A. Ueda, J. Electrochem. Soc. 141 (1994) 2972.
[5] T. Ohzuku, A. Ueda, N. Nagayama, Y. Iwakoshi, H. Komori, Electrochim. Acta 38 (1993) 159.
[6] T. Ohzuku, H. Tomura, K. Sawai, J. Electrochem. Soc. 144 (1997) 3496.
[7] J.N. Reimers, J.R. Dahn, Phys. Rev. B 47 (1993) 2995.
[8] A. van der Ven, M.K. Aydinol, G. Ceder, Phys. Rev. B 58 (1998) 2975.
[9] J.M. Rosolen, P. Ballirano, M. Berrettoni, F. Decker, M. Gregorkiewitz, Ionics 4 (1997) 345.
[10] E. Rossen, J.N. Reimers, J.R. Dahn, Solid State Ion. 62 (1993) 53.

[11] M. Yoshio, H. Tanaka, K. Tominaga, H. Noguchi, J. Power Sources 40 (1992) 347.
[12] H. Wang, Y.-H. Jang, B. Huang, D.R. Sadoway, Y.-M. Chiang, J. Electrochem. Soc. 146 (1999) 473.
[13] S.P. Sheu, C.Y. Yao, J.M. Chen, Y.C. Chiou, J. Power Sources 68 (1997) 533.
[14] A. Honders, J. Kinderen, A.H. Heeren, G.H.J. Broers, Solid State Ion. 14 (1984) 205.
[15] L.A. Montoro, M. Abbate, J.M. Rosolen, Electrochem. Solid-State Lett. 3 (2000) 416.
[16] L.A. Montoro, M. Abbate, E.C. Almeida, J.M. Rosolen, Chem. Phys. Lett. 309 (1999) 14.
[17] C. Wolverton, A. Zunger, Phys. Rev. Lett. 81 (1998) 606.
[18] R. Alcantara, P. Lavela, J.L. Tirado, E. Zhecheva, R. Stoyanova, J. Electroanal. Chem. 454 (1998) 173.
[19] J.M. Rosolen, F. Decker, J. Electroanal. Chem. 501 (2001) 253.
[20] H. Chen, X. Qiu, W. Zhu, P. Hagenmuller, Electrochem. Commun. 4 (2002) 488.
[21] D. Caurant, N. Baffier, B. Garcia, J.P. Pereira-Ramos, Solid State Ion. 91 (1996) 45.
[22] T. Takada, H. Hayakawa, E. Akiba, F. Izumi, B.C. Chakoumakos, J. Power Sources 68 (1997) 613.
[23] Y. Fujita, K. Amine, J. Maruta, H. Yasuda, J. Power Sources 68 (1997) 126.
[24] G.T.K. Fey, K.S. Chen, B.J. Hwang, Y.L. Lin, J. Power Sources 68 (1997) 519.
[25] Y.-M. Chang, Y.-I. Jang, H. Wang, B. Huang, D.R. Sadoway, P. Ye, J. Electrochem. Soc. 145 (1998) 887.
[26] R.J. Gummow, D.C. Liles, M.M. Thackeray, Mater. Res. Bull. 28 (1993) 1177.
[27] T.M.T.N. Tennakoon, G. Lindbergh, B. Bergman, J. Electrochem. Soc. 144 (1997) 2296.
[28] P.N. Kumta, D. Gallet, A. Waghray, G.E. Blomgren, M.P. Setter, J. Power Sources 72 (1998) 91.
[29] D. Larcher, M.R. Palacin, G.G. Amatucci, J.M. Tarascon, J. Electrochem. Soc. 144 (1997) 408.
[30] C.H. Chen, E.M. Kelder, M.J.G. Jak, J. Schoonman, Solid State Ion. 86 (1996) 1301.
[31] Z.S. Peng, C.R. Wan, C.Y. Jiang, J. Power Sources 72 (1998) 215.
[32] G.G.G. Amatucci, J.M. Tarascon, D. Larcher, L.C. Klein, Solid State Ion. 84 (1996) 169.
[33] B. Garcia, J. Farcy, J.P. Pereira-Ramos, J. Perichon, N. Baffier, J. Power Sources 54 (1995) 373.
[34] P.N. Kumta, D. Gallet, A. Waghray, G.E. Blomgren, M.P. Setter, J. Power Sources 72 (1998) 91.
[35] C.Y. Kuo, Solid State Technol. 17 (1974) 49.
[36] R.W. Vest, Ferroelectrics 102 (1990) 53.
[37] G.M. West, S. Singaram, Mat. Res. Soc. Symp. Proc. 60 (1986) 35.
[38] R.J. Gummow, M.M. Thackeray, W.I.F. David, S. Hull, MRS Bull. 27 (1992) 327.
[39] J.M. Rosolen, F. Decker, J. Electrochem. Soc. 143 (1996) 2417.
[40] J.K. Hong, J.H. Lee, S.M. Oh, J. Power Sources 111 (2002) 90.